Available online at www.sciencedirect.com

SCIENCE DIRECT®

Thin Solid Films 469–470 (2004) 377–382

thin solid films

www.elsevier.com/locate/tsf

Study on etching profile of nanoporous silica

C.W. Chen[a], T.C. Chang[b,c,*], P.T. Liu[d,e], T.M. Tsai[a], H.H. Wu[b], T.Y. Tseng[a]

[a]*Institute of Electronics, National Chiao Tung University, Hsin-Chu, Taiwan*
[b]*Department of Physics and Institute of Electro-Optical Engineering, National Sun Yat-Sen University, 70 Lien-hai Rd., 804 Kaohsiung, Taiwan*
[c]*Center for Nanoscience and Nanotechnology, National Sun Yat-Sen University, Kaohsiung, Taiwan*
[d]*National Nano Device Laboratories, 1001-1 Ta-Hsueh Road, Hsin-Chu 300, Taiwan*
[e]*Department of Photonics and Display Institute, National Chiao Tung University, Hsin-Chu, Taiwan*

Abstract

We have investigated the impact of H_2-plasma treatment on porous organosilicate glass (POSG) with etching process. The etching rate of trenches of nanoporous silica film was about 650 nm/min using fluorocarbon plasma. It is 1.6 times the etching rate of CVD oxide for the same etching condition due to the high porosity of POSG. We found that the profile of the intrinsic sample had mask undercutting. By the contrary, the mask undercutting effect was suppressed in the H_2-plasma-treated sample. Based on the FTIR spectra analysis, the Si–H bonding was appeared after H_2-plasma treatment. The existence of Si–H bonds enhances to possess high C/F ratio and high polymerization rate at the sidewall surface. As a result, the spontaneous reactive etching at sidewall was suppressed. We also observed the pattern profile of porous silica was distorted after O_2-plasma ashing. This is due to the oxidation of hydrophobic groups and the formation of Si–OH bonds in the bulk. The interaction between the siloxanol groups and the gelation reaction occurred in the internal of porous organosilicates predominate stress evolution, leading to the deformation of patterned porous organosilicate films.

Keywords: Dielectrics; Stress; Surface morphology

1. Introduction

It has been widely accepted that developing interlayer dielectrics (ILD) with low dielectric constant (low-*k*) for on-chip interconnects can effectively reduce resistance–capacitance (RC) delay and the power dissipation [1,2]. As feature sizes in integrated circuits (IC) approach 0.1 μm and beyond, specially, it is necessary to reduce the dielectric constant of the ILD layers below 2.2. The effective approach to achieve the ultralow-*k* demand is to incorporate nanoscale pores into the dielectric materials [3–5]. Among various porous low-*k* dielectrics, nanoporous organosilica glasses (POSGs) are receiving much attention on ILD applications [6–8]. Their adjustable dielectric properties make the nanoporous silicate suitable for different IC technology nodes. Nevertheless, the adoption of POSGs encounters difficulties in IC integration processing due to their large internal surfaces. The high porosity in their structures tends to adsorbing environmental contaminants, such as moisture [9]. The weak resistance of porous low-*k* against the reactive plasma and stripper is troublesome for integration with Cu. The dual damascene is the standard structure for Cu metallization [10]. This approach combines the fabrication of metal wires and studs. It is needed to produce the trench and via structures on dielectrics prior to metal deposition and CMP steps. The required patterns transferring to dielectric thin films are fabricated by lithography and plasma etching techniques. However, the low-*k* materials meet some troubles during the conventional pattern sequence. Comparing with SiO_2 deposited by CVD, POSG was low density and sensitive due to its high porosity and high surface/volume ratio [11].The resultant electrical degradation of organosilicate-based porous materials has been proposed in previous researches

* Corresponding author. Department of Physics and Institute of Electro-Optical Engineering, National Sun Yat-Sen University, 70 Lien-hai Rd., 804 Kaohsiung, Taiwan. Tel.: +7 525 2000x3708; fax: +3 572271.
E-mail address: tcchang@mail.phys.nsysu.edu.tw (T.C. Chang).

0040-6090/$ - see front matter © 2004 Published by Elsevier B.V.
doi:10.1016/j.tsf.2004.08.154

[12,13].The impacts of etching and photoresist stripping with plasma on the integrity of pattern profiles have not been widely explored yet. In addition, stress development of POSGs after O_2-plasma ashing has not been completely clear during thermal cycles in IC processes.

In this work, we study a nanoporous organosilica film (k=1.9) with structural porosity of 50%, manufactured by Chemat Technology [12]. This kind of POSG film is based on methyl silsesquioxane [MSSQ, $(RSiO_{1.5})_n$, R: organic substituent] matrix, except it contains CH_x (x=1−2) bridging the siloxane networks (–Si–O–Si–). This molecularly three-dimensional bonded matrix of the POSG offers potential improvements in the mechanical strength relative to silica xero- and aerogels [9]. For practical process integration considerations, the impact of etching and photoresist stripping on the POSG film is discussed first. Film residual stress measurement is performed during a thermal cycle to investigate the pattern distortion and stress development in the POSG film.

2. Experimental details

Methyl silsesquioxane resin as the matrix material, which is low molecular weight with a large number of $Si(OH)_x$ and $Si(OC_2H_5)_x$ (x=1–4) groups, was formulated to 30 wt.% solids in a carrier solvent of methylisobutylketone. Poly (methylmethacrylate) polymers (PMMA) with 20 wt.% loading, working as foaming agents, were subsequently added in the MSSQ matrix material to ultimately produce porous organosilicates. As most of PMMA polymers were compatible with MSSQ, a uniform precursor solution of the mixture was obtained immediately. For fabricating porous organosilicate films, the precursor solution was first spin-coated onto a 6-in. p-type wafers with (100) orientation. The first-stage spin rate was 450 rpm for 4 s, and the second 3000 rpm for 30 s, respectively. The resultant wafers were transferred to a quartz furnace and heated up from room temperature to 425 °C at a ramping rate of 20 °C/min. A thermal curing process was then proceeding at 425 °C for 1 h under nitrogen atmosphere, and further forming the POSG films with a thickness of 500 nm.

The H_2-plasma treatments of POSG films were performed in the PECVD chamber with RF power 100 W at a pressure of 500 m Torr. The H_2 flow rate was 400 sccm, and the operated temperature was kept at 250 °C. The trench patterns were formed by etching through the POSG films down to the surface of Si substrates in a high-density plasma etch tool (Anelva ILD-4100 helicon wave etcher), operating in the 1.5 mTorr pressure. The etchant chemistries were CHF_3 and CF_4 with a gas flow rate of 20 sccm and RF power 800 W. The removal of photoresist was in situ performed using O_2-plasma ashing process in the Anelva etcher. The process conditions of O_2-plasma ashing were as follows, gas flow rate of 200 sccm, and RF power of 1000 W, and the processing time was varied ranging from 20 to 40 s. The pattern profiles of etched POSG films were imaged by the scanning electron microscopy (SEM). To explore the physical mechanism for experimental findings, the measurement of film residual stress was conducted on another group of blanket POSG films with and without O_2-plasma exposure, respectively. The relation between residual stresses versus temperatures up to 360 °C was measured by the wafer curvature method [14] at a TENCOR thin-film stress measure system. Also, the films were characterized by Fourier transform infrared spectroscopy (FTIR).

3. Results and discussion

The etching rate of trench patterns for the POSG films was about 650 nm/min, 1.6 times the etching rate of typical chemical vapor deposition (CVD) silicon dioxide under the same etching conditions. This result is expected due to the high porosity of POSG films. Fig. 1(a) and (b) show the etching profiles which were made with the same plasma condition but not proceeded the O_2-plasma ashing process. The photoresist was still capping on the POSG films. The POSG film in Fig. 1(b) was treated by H_2-plasma for 5 min before the etching process, the other one showed in Fig. 1(a)

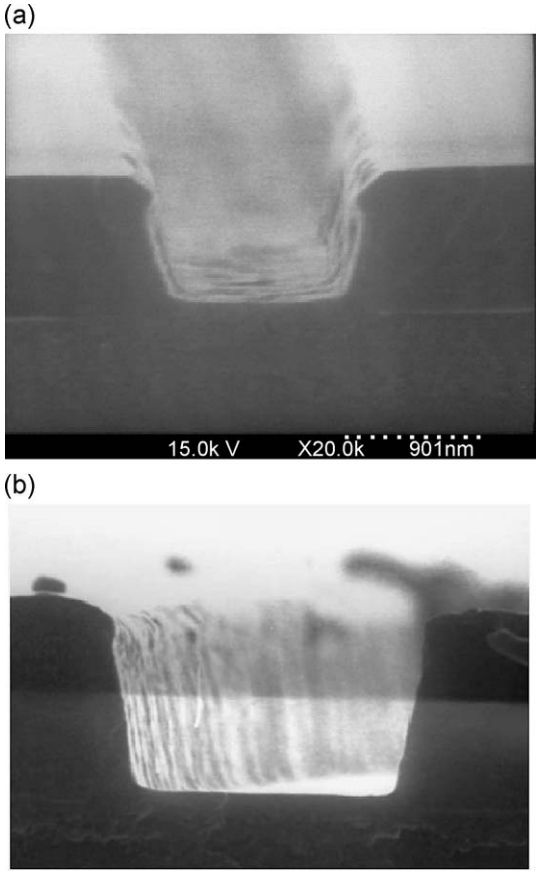

Fig. 1. Cross-sectional profiles of POSG films after pattern transfer processes. (a) The mask undercutting was observed in intrinsic films. (b) The mask undercutting was suppressed in H_2-treated films.

was untreated. Keeping eyes on the sidewall surface, we can find that the profile of the untreated film has mask undercutting. By the contrary, the profile of the H_2-plasma-treated film does not have mask undercutting. The different characteristic in the sidewall was believed due to fluorocarbon polymer formation which could control the etching rate. Standaert et al. [15] have observed that high density fluorocarbon plasmas could form a thick steady-state fluorocarbon polymer layer on the surface of films during the etching process. The etching rate at the sidewall was controlled by the thickness of the polymer, which influenced the incident ion fluxes and their energies on the plasma–surface interaction [16]. If straight sidewalls are desired, a suitable fluorocarbon polymer must be formed and must suppress the spontaneous etching at the sidewall. The thickness and composition of carbon-related polymer is determined by plasma chemistries, RF power, temperature, and C/F ratio. High C/F ratio of plasma at surface results a thicker polymer layer. H, C, F contained in the oxide-based films would also affect the polymerization due to different C/F ratio at the surface [17]. Hydrogen containing oxide-based films would have high polymerization and low etching rate. The enlargements of Si–H bonding at 2250 cm^{-1} in the FTIR spectra for the intrinsic and H_2-plasma-treated sample were shown in Fig. 2. Comparing with both samples, the distinct appearance of Si–H bonding in the H_2-treated sample was observed. It is obvious that the formation of Si–H bonds due to the H_2-plasma treatment would enhance to possess high C/F ratio and high polymerization rate at the sidewall surface. As a result, the spontaneous reactive etching at the sidewall and mask undercutting were suppressed as shown in Fig. 1(b).

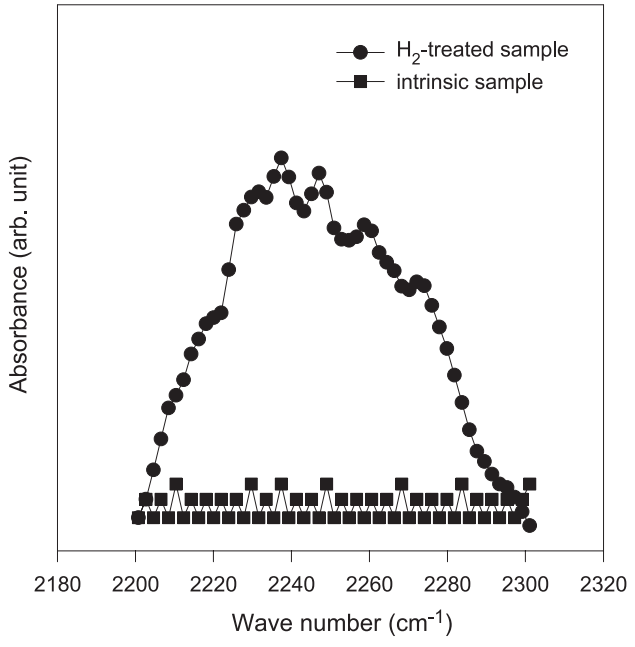

Fig. 2. The enlargements of Si–H bonding at 2250 cm^{-1} in FTIR spectra for the intrinsic and H_2-treated samples. The distinct Si–H bonding was formed after H_2-plasma treatment.

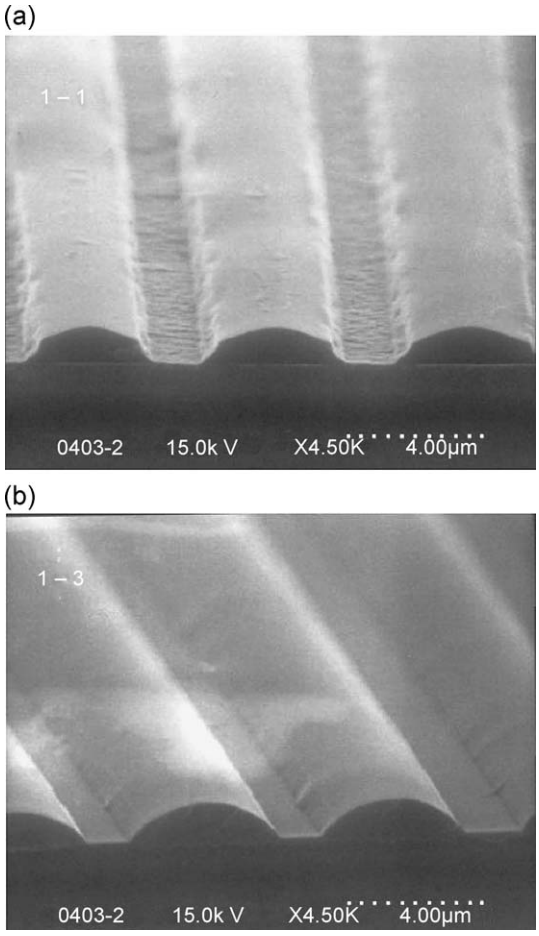

Fig. 3. (a) SEM micrographies of patterned POSG films after photoresist stripping with O_2-plasma exposure for 20 s, and (b) for 40 s. The etching profiles of POSG films are distorted significantly after photoresist removal.

Fig. 3(a) and (b) show, after photoresist stripping, the etching profiles of POSG films are distorted significantly after photoresist removal. With the increase of O_2-plasma ashing periods from 20 to 40 s, the degree of pattern distortion is even getting worse. For further investigation on the pattern deformation, FTIR analysis and residual stress measurement of the POSG films were performed. Fig. 4 shows FTIR spectra of the POSG films before and after O_2-plasma ashing for 20 and 40 s, respectively. For the as-cured POSG film (i.e., POSG without O_2-plasma exposure), main function groups indicated in the FTIR spectrum are the Si–C stretch peaks (at 781, 1273 cm^{-1}), Si–O stretch modes (network-like vibration at near 1070 cm^{-1}, cagelike vibration at near 1130 cm^{-1}), and C–H peak (at 2975 cm^{-1}). Among these main function groups, Si–C and C–H groups are hydrophobic, which will make both of the film surfaces and internal pores hydrophobic, minimizing moisture uptake in films. Nevertheless, it is observed after O_2-plasma ashing, the peak intensities of Si–C and C–H bonds are reduced significantly, and new peaks of Si–OH bond (at 945 cm^{-1}) and Si–OH mixed with H–OH bonds (at around 3300–3600 cm^{-1}) appear. This observation indicates, after photoresist stripping with

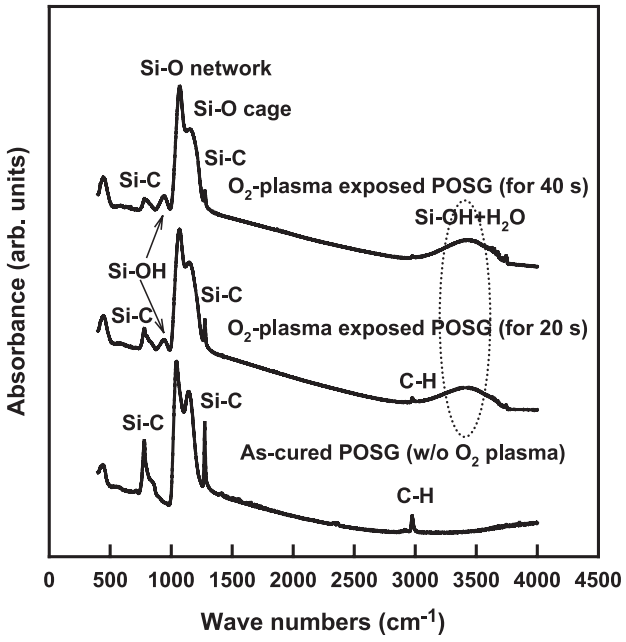

Fig. 4. FTIR spectra of POSG films before and after O_2-plasma ashing for 20 and 40 s.

O_2-plasma exposure, plenty of organic function groups are destroyed, resulting in increasing dangling bonds in the POSG film. This is more possible for the highly porous structure. Some of those dangling bonds may form Si–O bonds, and others convert into Si–OH bonds [18]; thereby, the POSG film absorbs moisture much more easily. The dielectric constant of POSG films after O_2-plasma processing increases from 1.9 to around 8.0 [12].

Fig. 5 displays, during a thermal cycle up to 360 °C, the stress evolution of POSG films before and after the O_2-plasma ashing process. In this work, maximum measurement temperature was limited at 360 °C due to the heat capacity of heater in our stress measure system. It is found that the POSG film has positive stress values on Si substrate, indicating the POSG film sustains tensile stress. Also, the change in stress of the as-cured POSG film is slight and exhibits a linear relationship with temperatures and displays no hysteresis behavior after the thermal cycle. In contrast, an obvious discrepancy and irreversible trend appears at the stress development of O_2-plasma-exposed POSG film during the thermal cycle. The residual stress in the silicate-based thin film, σ_s, could divided into three components [19].

$$\sigma_s = \sigma_i + \sigma_{th} + \sigma_w$$

σ_i is intrinsic stress which is related to the composition and deposition condition of the film. σ_{th} is the term of thermal stress due to the difference of the expansion coefficient of the substrate and thin film. The final term, σ_w, is water-induced (or extrinsic) stress result from interactions between the film and the environment [19]. Among the three contributions, the evolution of both intrinsic stress and thermal stress is reversible, while extrinsic stress development is irreversible during thermal cycles. In Fig. 5 for the POSG without O_2-plasma exposure, the reversibility of stress versus temperature curve right shows the as-cured POSG film possesses elastic behavior and is thermally stable beyond 360 °C, at least. However, the inconsistency of stress behavior in the O_2-plasma-exposed POSG film can be deduced further in view of the residual stresses at points A, B, C, and D in Fig. 5, respectively. It is first observed by comparing points B with A that the tensile stress of O_2-plasma-exposed POSG film is about two times larger than that of the as-cured one at room temperature. This result is mainly due to the fact that characteristic function bonds in the POSG films are modified after photoresist stripping. As previously shown in Fig. 4, Si–CH_3 groups are removed by O_2-plasma oxidation, accompanied by a simultaneous increase of the Si–OH content in the O_2-plasma-exposed POSG. Owing to the hydrogen bonding of Si–OH groups, each Si–OH groups in the organosilicate film will attract each other [20]. This interaction between siloxanol groups [$Si(OH)_n$, n=1−4] leads the organosilicate radicals to shrinkage so that the tensile stress increases [21,22]. Such increase in tensile stress and partly due to surface energy minimization are responsible for pattern profile distortion of POSG films after photoresist stripping. This phenomenon of pattern distortion is especially significant with increasing O_2-plasma ashing periods, as anteriorly shown in Fig. 3a and b. Furthermore, by comparing points B with C, the intensity of tensile stress

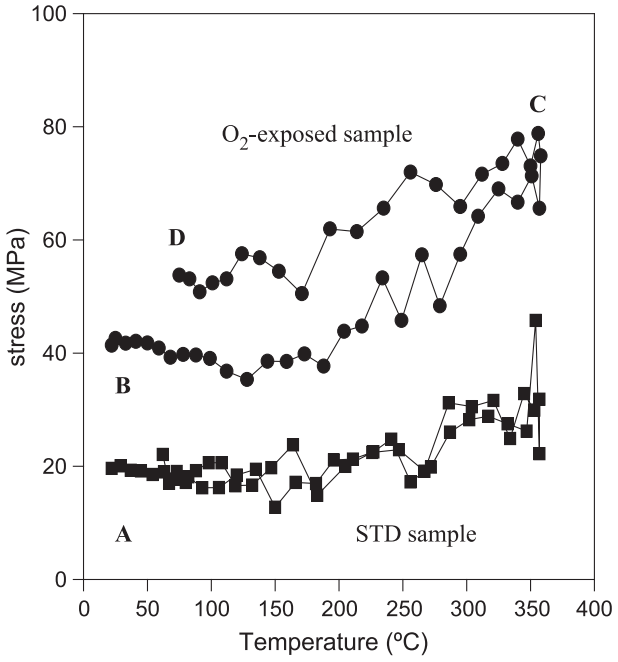

Fig. 5. Dependence of residual stress on temperature for POSG films before and after O_2-plasma ashing for 20 s during a thermal cycle up to 360 °C. Points A, B, C, and D denote the residual stresses of POSG films measured at different conditions separately. Point A: the as-cured POSG (without O_2-plasma exposure) measured at room temperature; point B: the O_2-plasma as-exposed POSG measured at room temperature; point C: the O_2-plasma-exposed POSG measured at 360 °C; and point D: the O_2-plasma-exposed POSG following the thermal cycle and measured at room temperature.

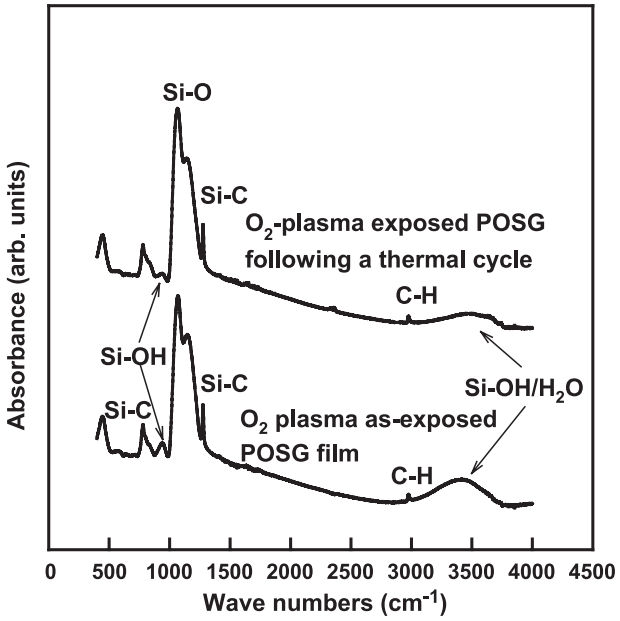

Fig. 6. Comparison of FTIR spectra for the O_2-plasma as-exposed POSG film (i.e., point B in Fig. 5) and the one following a thermal cycle up to 360 °C (i.e., point D in Fig. 5).

in O_2-plasma-exposed POSG film continues to increase as the temperatures of measurement are increased. This origin of increasing tensile stress is attributed to the film gelation and dehydration reactions which occurred in the O_2-plasma-exposed POSG film during the temperature rising, via the following chemical reactions:

$$\equiv SiOH + SiOH\equiv \rightarrow \equiv Si - O\equiv + H_2O$$

The chemical events will also lead to the significant film shrinkage and inevitably induce pattern distortion of POSG films and stack layer peeling potentially. Subsequently, relaxation of the tensile stress takes place irreversibly during the temperature cooling (from points C to D), originating from moisture readsorbing into the POSG film under atmosphere. Because previously occurred gelation reactions reduce Si–OH content in the POSG film, leading to less moisture uptake (~3450 cm^{-1}) at the state of point D in comparison with point B, the relaxation of tensile stress will not come back to the same state as point B. FTIR spectra shown in Fig. 6 confirm our inference. It indicates that the intensities of Si–OH and Si–OH/H_2O in the POSG film experienced an entire thermal cycle (i.e., point D) are much lower than those in the O_2-plasma as-exposed POSG film (i.e., point B). Thus, the stress evolution in the O_2-plasma-exposed POSG film is irreversible and displays a hysteresis behavior following the entire thermal cycle.

4. Conclusions

The etching and photoresist stripping of nanoporous organosilicate are studied in a high-density inductively coupled plasma reactor. The etching rate of trench patterns for the POSG films was about 650 nm/min, 1.6 times the etching rate of CVD silicon dioxide, using fluorocarbon plasma. The Si–H bonding appeared in the POSG after H_2-plasma treatment in PECVD and suppressed the mask undercutting during the etching process. This is because the existence of Si–H bonds leads to high C/F ratio and high polymerization rate at the sidewall surface. In addition, pattern profile distortion and stress evolution of nanoporous organosilicate exposed to O_2-plasma have been observed during a thermal cycle up to 360 °C. The initial residual stresses of the as-cured POSG film are tensile and exhibit reversible behavior in a stress versus temperature curve. After photoresist stripping, however, tensile stresses increase significantly in the POSG film due to a consequence of the hydration of porous silicate exposed to O_2-plasma ambience. This result leads to POSG film shrinkage and pattern profile deformation. In addition, further gelation reactions in the O_2-plasma-exposed POSG film will enhance progressively the intensity of tensile stresses with increasing measurement temperatures. On the basis of these reaction mechanisms, irreversible behavior of residual stresses in stress versus temperature curve can be well deduced for the POSG film after photoresist stripping.

Acknowledgement

This work was performed at the National Nano Device Laboratory and was supported by the United Microelectronic, the Chemat and the National Science Council of the Republic of China under Contract No. NSC92-2112-M-110-020.

References

[1] T.E. Seidel, C.H. Ting, Mater. Res. Soc. Symp. Proc. 381 (1995) 3.
[2] International Technology Roadmap for Semiconductors (ITRS), 2001 November, Santa Clara, CA.
[3] C. Jin, J.D. Luttmer, D.M. Smith, T.A. Ramos, Mater. Res. Soc. Bull. 22 (1997) 39.
[4] Y. Lu, R. Ganguli, C.A. Drewen, M.T. Anderson, C.J. Brinker, Nature 389 (1997) 364.
[5] J.H. Golden, C.J. Hawker, P.S. Ho, Semiconductor International (2001 May).
[6] P.A. Kohl, Q. Zhao, K. Patel, D. Schmidt, S.A. Bidstrup-Allen, R. Shick, S. Jayaraman, Proceedings of the 3rd international Symposium on Low and High Dielectric Constant Materials, The Electrochem. Soc., vol. 98-3, 1998, p. 169.
[7] P.A. Kohl, A. Padovani, M. Wedlake, D. Bhusari, S.A.B. Allen, R. Shick, L. Rhodes, Mater. Res. Soc. Symp. Proc. 565 (1999) 55.
[8] J. Liu, D. Gan, C. Hu, M. Kiene, P.S. Ho, W. Volksen, R.D. Miller, Appl. Phys. Lett. 81 (2002) 4180.
[9] R.D. Miller, R. Beyers, K.R. Carter, R.F. Cook, M. Harbison, C.J. Hawker, J.L. Hedrick, V. Lee, E. Liniger, C. Nguyen, J. Remenar, M. Sherwood, M. Trollsas, W. Volksen, D.Y. Yoon, Mater. Res. Soc. Symp. Proc. 565 (1999) 3.
[10] J. Torres, Proc. 1999 IEEE IITC, 1999, p. 253.
[11] T.C. Chang, C.W. Chen, P.T. Liu, Y.S. Mor, H.M. Tsai, T.M. Tsai, S.T. Yan, C.H. Tu, T.Y. Tseng, S.M. Sze, Electrochem. Solid-State Lett. 6 (2003) F13.

[12] P.T. Liu, T.C. Chang, Y.S. Mor, C.W. Chen, T.M. Tsai, C.J. Chu, F.M. Pan, S.M. Sze, Electrochem. Solid-State Lett. 5 (2002) G11.
[13] Y.S. Mor, T.C. Chang, P.T. Liu, T.M. Tsai, C.W. Chen, S.T. Yan, C.J. Chu, W.F. Wu, F.M. Pan, W. Lur, S.M. Sze, J. Vac. Sci.Technol., B 20 (2002) 1334.
[14] R.J. Jaccodine, W.A. Schlegel, J. Appl. Phys. 37 (1966) 2429.
[15] T.E.F.M. Standaert, M. Schaepkens, N.R. Rueger, P.G.M. Sebel, G.S. Oehrlein, J.M. Cook, J. Vac. Sci. Technol., A, Vac. Surf. Films 16 (1) (1998) 239.
[16] G.S. Oehrlein, Y. Kurogi, Mater. Sci. Eng. 24 (1998) 153.
[17] T.E.F.M. Standaert, P.J. Matsuo, S.D. Allen, G.S. Oehrlein, T.J. Dalton, J. Vac. Sci. Technol., A, Vac. Surf. Films 17 (3) (1999) 741.
[18] T. Furusawa, D. Ryuzaki, R. Yoneyama, Y. Homma, K. Hinode, Electrochem. Solid-State Lett. 4 (2001) G31.
[19] H. Leplan, B. Geenen, J.Y. Robic, Y. Pauleau, J. Appl. Phys. 78 (1995) 962.
[20] R.K. Iler, The Chemistry of Silica, Wiley, New York, 1979.
[21] E. Kondoh, T. Asano, A. Nakashima, M. Komatu, J. Vac. Sci. Technol., B 18 (2000) 1276.
[22] E. Kondoh, M.R. Baklanov, H. Bender, K. Maex, Electrochem. Solid-State Lett. 2 (1998) 224.